INFECTION AND IMMUNITY, Sept. 2008, p. 4332–4344 Vol. 76, No. 9
0019-9567/08/$08.00+0 doi:10.1128/IAI.00278-08

Inhibition of Malaria Parasite Development by a Cyclic Peptide That Targets the Vital Parasite Protein SERA5▽

W. Douglas Fairlie,[1]† Tim P. Spurck,[2]† Joanne E. McCoubrie,[1] Paul R. Gilson,[1] Susanne K. Miller,[1] Geoffrey I. McFadden,[2] Robyn Malby,[1] Brendan S. Crabb,[1] and Anthony N. Hodder[1]*

The Walter and Eliza Hall Institute of Medical Research, 1G Royal Parade, Parkville, Victoria 3050, Australia,[1] and The School of Botany, The University of Melbourne, Grattan St., Parkville, Victoria 3010, Australia[2]

Received 28 February 2008/Returned for modification 30 March 2008/Accepted 20 June 2008

The serine repeat antigen (SERA) proteins of the malaria parasites *Plasmodium* spp. contain a putative enzyme domain similar to that of papain family cysteine proteases. In *Plasmodium falciparum* parasites, more than half of the SERA family proteins, including the most abundantly expressed form, SERA5, have a cysteine-to-serine substitution within the putative catalytic triad of the active site. Although SERA5 is required for blood-stage parasite survival, the occurrence of a noncanonical catalytic triad casts doubt on the importance of the enzyme domain in this function. We used phage display to identify a small (14-residue) disulfide-bonded cyclic peptide (SBP1) that targets the enzyme domain of SERA5. Biochemical characterization of the interaction shows that it is dependent on the conformation of both the peptide and protein. Addition of this peptide to parasite cultures compromised development of late-stage parasites compared to that of control parasites or those incubated with equivalent amounts of the carboxymethylated peptide. This effect was similar in two different strains of *P. falciparum* as well as in a transgenic strain where the gene encoding the related serine-type parasitophorous vacuole protein SERA4 was deleted. In compromised parasites, the SBP1 peptide crosses both the erythrocyte and parasitophorous vacuole membranes and accumulates within the parasitophorous vacuole. In addition, both SBP1 and SERA5 were identified in the parasite cytosol, indicating that the plasma membrane of the parasite was compromised as a result of SBP1 treatment. These data implicate an important role for SERA5 in the regulation of the intraerythrocytic development of late-stage parasites and as a target for drug development.

Malaria remains one of the most devastating diseases of mankind, inflicting serious health and economic burdens on many countries throughout the world. *Plasmodium falciparum* is responsible for the most acute form of the disease and is directly responsible for the death of more than 1 million children under the age of 5 years annually (www.who.int/health_topics/malaria) (37). Recently, the effective control of both the *Anopheles* sp. vector and the *Plasmodium* sp. parasite has been hindered by the emergence of resistance to treatments with insecticides and prophylactic drugs, respectively (10, 20, 40, 41). Hence, an effective vaccine and new drugs to treat the disease are urgently required. One family of proteins with the potential to serve as targets for both vaccines and therapeutic compounds are the blood-stage serine repeat antigens (SERAs) (8, 14, 24).

There are nine genes in the *sera* family in *P. falciparum*. Eight are located in a head-to-tail cluster on chromosome 2, while one is on chromosome 9 (9, 16, 17). In cultured parasites, only those *sera* genes with low or absent expression can be disrupted, indicating that not all members of this multigene family are essential for blood-stage growth (3, 30). SERA5 and -6 appear to be the most important SERAs in various strains of *P. falciparum* blood-stage parasites because they are expressed at higher levels than most family members and all attempts to disrupt these genes have, to date, been unsuccessful (3, 30).

The SERA proteins are synthesized as ~120-kDa precursors in late trophozoites (12, 14, 24), with a signal peptide that is cleaved upon translocation through the endoplasmic reticulum (33) and then exported into the lumen of the parasitophorous vacuole (8). The precursor molecule is processed into N-terminal 47-kDa, central 56-kDa, and C-terminal 18-kDa fragments at about the time of schizont rupture and merozoite release (Fig. 1). The 47-kDa and 18-kDa fragments remain covalently linked via at least a single disulfide bond, while the 56-kDa fragment undergoes further processing to a 50-kDa species that can be inhibited by the cysteine protease inhibitors leupeptin and E64 (11, 12, 14, 26).

The C-terminal end of the central domain of all SERA proteins shows approximately 20% sequence identity to the papain family of cysteine proteases (8, 18, 23). Curiously, six of the nine *P. falciparum* SERAs (SERA1 to -5 and SERA9) have a cysteine-to-serine replacement within the putative catalytic triad; the remaining three SERAs (SERA6 to -8) have the canonical cysteine as the active-site residue. The noncanonical serine substitution has provoked debate as to whether or not the SERAs with an active-site serine are capable of a physiological enzymatic function (23), even though unusual catalytic triads have been described for *P. falciparum* as well as other organisms (4, 6, 27, 35, 43). Importantly, we recently demonstrated that the recombinant enzyme domain of *P. falciparum* SERA5, a "serine-type" SERA, has a chymotrypsin-like activity (22). This activity was observed at pH 7.5, but not pH 5.5,

* Corresponding author. Mailing address: Division of Infection and Immunity, The Walter and Eliza Hall Institute of Medical Research, 1G Royal Parade, Parkville, Victoria, Australia 3050. Phone: 61 3 9345 2555. Fax: 61 3 9347 0852. E-mail: hodder@wehi.edu.au.

† W.D.F. and T.P.S. contributed equally to the manuscript.

▽ Published ahead of print on 30 June 2008.

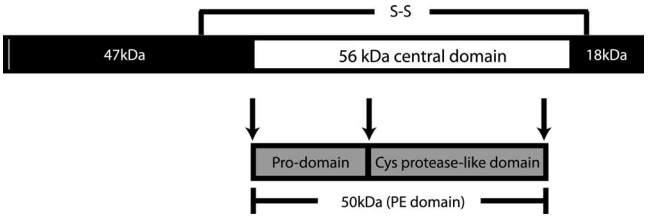

FIG. 1. Schematic of full-length SERA5 protein. The location of the 50-kDa central domain fragment containing the proenzyme (PE) domain (residues T391 to N828) and the enzyme (E) domain (residues V544 to N828) is indicated.

and can be prevented by the addition of the serine protease inhibitor 3,4-dichloroisocoumarin (22).

Although gene disruption studies indicate an essential role for SERA5 and SERA6, their exact function in the parasite blood stage is still unclear. Since genetic deletion of these important proteins is not feasible, other approaches to determining their roles are required. Here we adopted phage display to identify a short cyclic peptide that binds to the enzyme domain of one of these essential SERAs, SERA5. The peptide colocalizes with SERA5 in the parasitophorous vacuole of trophozoites and schizonts and arrests late-stage parasite development. These data provide the first evidence that a relatively small molecule can disrupt the function of the SERA proteins and identify a lead compound for the design of small-molecule peptidomimetic antimalarial drugs.

MATERIALS AND METHODS

Chemicals. All chemicals were purchased from Sigma unless otherwise specified.

Proteins, peptides, and antibodies. The SERA5 proenzyme domain (SERA5PE), SERA5 enzyme domain (SERA5E) (see Fig. 1 for a description of these constructs), and SERA4 proenzyme domain (SERA4PE; residues T309 to E726) were expressed in *Escherichia coli* and purified following refolding from inclusion bodies as described previously (22). The reduced and alkylated proteins were produced by incubation with 20 mM dithiothreitol for 60 min at 45°C followed by addition of iodoacetic acid to a final concentration of 100 mM. After incubation in the dark at room temperature for 1 h, the carboxymethylated proteins were purified by reversed-phase high-performance liquid chromatography (RP-HPLC) on a C_8 Vydac column equilibrated in 0.1% (vol/vol) trifluoroacetic acid (TFA) and eluted with a 40-min gradient of 0 to 80% (vol/vol) acetonitrile in 0.09% (vol/vol) TFA. Collected fractions containing the modified protein were pooled, lyophilized, and then solubilized in phosphate-buffered saline (PBS) or 10× RPMI-HEPES. Cyclized SERA5 binding peptide (SBP1) (LVCHPAV PALLCAR) containing an intramolecular disulfide bond was purchased from Auspep Pty. Ltd. (Melbourne, Australia). A reduced and alkylated form of the peptide was prepared as described above for the reduced and alkylated proteins, and the modification was confirmed by matrix-assisted laser desorption ionization–time-of-flight mass spectrometry. The cyclized SBP1 was biotinylated using *N*-hydroxysuccinimide–biotin per the manufacturer's procedure (Pierce), and the modification was confirmed using matrix-assisted laser desorption ionization–time-of-flight mass spectrometry.

Antibodies raised to SERA5E and SERA5PE were produced by the Walter and Eliza Hall Institute antibody production facility. All antibody preparations were affinity purified using protein G resins (Amersham Biosciences), buffer exchanged into PBS, and sterile filtered prior to use. The specificity of the monoclonal antibodies (MAbs) for SERA5 was validated using immunoblots of late-stage *P. falciparum* strain 3D7 schizonts.

Sodium dodecyl sulfate-polyacrylamide gel electrophoresis (SDS-PAGE) and immunoblotting of proteins. Sorbitol-synchronized *P. falciparum* 3D7 schizonts (~5% parasitemia) were purified using a Miltenyi Biotec Vario MACS CS magnetic separation column. Whole parasites were washed in PBS prior to solubilization in sample buffer, with or without β-mercaptoethanol. Parasite and recombinant proteins were fractionated in 4 to 12% bis-Tris precast gels (Invitrogen) and electrophoretically transferred onto a 0.2-μm polyvinylidene difluoride membrane. Immunoblotting was performed using previously described procedures (22).

Construction of phage display libraries. Two sets of phage-displayed random peptide libraries were constructed for panning against SERA5. One set consisted of 14-residue peptides with either all residues randomized (linear libraries) or all residues randomized in the context of a pair of fixed cysteine residues (cyclic libraries). These libraries are identical to those described previously with peptides fused to the M13 gene VIII coat protein (15) and were prepared essentially as described by Sidhu et al. (36). The second set of libraries was similarly constructed, except that the libraries consisted of eight-residue peptides, both linear and cyclic. In the cyclic libraries, the spacing of the cysteine residues varied from three to six residues. The randomization of residues for both sets of libraries was achieved using Kunkel mutagenesis (25), employing degenerate oligonucleotides in which each randomized residue was encoded by an NNS codon. Equal aliquots of each linear and cyclic sublibrary for each peptide length were combined, giving rise to two (8- and 14-residue) pools prior to panning against SERA5.

Panning of libraries against SERA5. SERA5E was incubated overnight at 4°C to coat five wells of a 96-well microtiter plate (Maxisorp; Nunc) at a concentration of 2 μg/ml in 100 μl PBS. After being washed with PBS containing 0.1% (vol/vol) Tween 20 (PBS-Tween 20), wells were blocked on alternate rounds with either 5% (wt/vol) bovine serum albumin (BSA) or 0.5% (wt/vol) casein for 1 h at room temperature. The libraries were then added (diluted 1:10 in PBS-Tween 20 containing either 0.1% BSA or 0.5% casein, corresponding to the blocking agent used) and incubated for 2 h at room temperature. The wells were then washed 15 times with PBS-Tween 20, and the phage were eluted by incubation with 0.1 M HCl for 3 min. After neutralization with 1 M Tris-HCl, pH 8.0, the phage were propagated by incubation overnight with *E. coli* XL-1 Blue and M13KO7 helper phage as described previously (15). After each round of panning, phage were isolated from cell supernatants by precipitation with polyethylene glycol-NaCl as described by Sidhu et al. (36).

Screening and sequencing of phage clones. Phage screening was performed exactly as described previously (15). Briefly, individual colonies obtained from infecting *E. coli* XL-1 Blue with phage from the final (sixth) round of panning were grown overnight with M13KO7 helper phage. The cell supernatants were then screened by enzyme-linked immunosorbent assay (ELISA), using immobilized SERA5E. Clones that gave the highest response with low background binding were then sequenced as described previously (15).

Competition ELISA. Prior to analysis of peptide binding affinities by phage ELISA, peptides of interest were displayed as gene III fusions following replacement of the gene VIII fragment with the corresponding fragment of the gene III display vector, as described previously (15). Competitive phage ELISAs were performed essentially as described previously (15), but SERA5 or peptides were used to displace phage-displayed peptide from binding to immobilized SERA5 protein. A 96-well plate was coated overnight at 4°C with 100 μl/well of SERA5E or SERA5PE at 2 μg/ml in PBS. After blocking of the plate for 90 min at room temperature with 200 μl/well of 6% (wt/vol) skim milk powder in PBS, M13 phage particles displaying SBP fused to M13 gene III were added to the wells at a subsaturating dilution, together with increasing concentrations of competitor in 100 μl of PBS-Tween 20 containing 1% (wt/vol) skim milk (PBS-Tween 20-milk). After 90 min of incubation at room temperature with shaking, the wells were washed 15 times with PBS-Tween 20, and an anti-M13 phage polyclonal antibody conjugated to horseradish peroxidase (Amersham Pharmacia) was added at 100 μl/well at a dilution of 1:2,000 in PBS-Tween 20-milk and incubated for 30 min at room temperature. The wells were then washed 15 times with PBS-Tween 20, and the substrate 3,3′,5,5′-tetramethylbenzidine–hydrogen peroxide (Kirkegaard & Perry Laboratories, Inc.) was added at 100 μl/well. The reaction was allowed to proceed for 10 min at room temperature, after which it was stopped by the addition of 50 μl/well of 2 M phosphoric acid. The absorbance at 450 nm was then read on a microtiter plate reader.

Parasite culture and growth assays. Parasite cultures and growth assays were performed as previously reported (21). Briefly, strains 3D7 and D10 and a *sera4* knockout mutant (a D10 derivative) (29) were grown as previously described (39), synchronized twice in sorbitol (1), and used at high initial trophozoite parasitemias (2 to 3%) to investigate the effect of the biotinylated or nonbiotinylated form of the SBP1 peptide on mature, blood-stage parasite development. Time intervals commenced as judged by the emergence of ring-stage parasites in control cultures containing PBS or the reduced and alkylated form of SBP1 as an additive. Unless specified otherwise, thin blood smears of parasites were visualized by light microscopy using Giemsa stain. Values represent the means and standard errors of the means (SEM) and were derived from at least triplicate independent experiments.

Confocal microscopy. Infected red blood cells were prepared as described previously (38). In brief, twice-synchronized cells were centrifuged at 1,500 rpm, and the remaining pellet was washed in RPMI-HEPES. Cells were then fixed with 4% electron microscopy (EM)-grade formaldehyde (Electron Microscopy Sciences) and 0.0075% EM-grade glutaraldehyde (Electron Microscopy Sciences) in RPMI for 1 hour (fixative concentrations were titrated to the lowest usable concentration of glutaraldehyde for each blood batch). Fixed cells were washed in PBS, permeabilized with 0.1% Triton X-100–PBS for 10 min, washed again in PBS, and then treated with ~0.1 mg/ml of sodium borohydride ($NaBH_4$)-PBS for 5 min. After being washed in PBS, cells were blocked in 3% BSA-PBS (blocking buffer) for approximately 30 min. Cells were incubated with the anti-SERA5 antibodies (diluted 1:500 in blocking buffer) or the biotinylated SBP1 peptide (33.5 μg/ml) and allowed to bind overnight at 4°C in 3% BSA-PBS. Following washing of the cells, the appropriate secondary antibody (either Alex Fluor 546–goat anti-mouse or -rabbit, Alexa Fluor 488–goat anti-mouse or -rabbit [Molecular Probes], or fluorescein isothiocyanate [FITC]-avidin [Zymed]) was added at a 1:1,000 dilution in blocking buffer and allowed to bind overnight at 4°C. Cells were then washed, incubated with 20 μg/ml Hoechst 33258 (Aldrich) in PBS for 5 min, and washed again in PBS, and then approximately 5 μl of cells was settled onto a previously flamed coverslip coated with 0.1% polyethylenimine briefly before the addition of an antifade mounting medium containing 70% glycerol-PBS with 0.1 mg/ml of 1,4-diazabicyclo[2.2.2]octane. Coverslips were inverted onto slides and sealed with petrolatum-lanolin-paraffin (1:1:1). Images were captured on a Leica TCS SP2 confocal microscope using an HCX PL APO 63/1.4 objective, and image stacks were processed using Leica SP2 software and subsequently arranged in Adobe Photoshop.

Semiquantitative analysis of fluorescence intensity was determined using Leica (SP2) analysis software. Briefly, for fluorescence calibration, a 488-nm argon laser was set to a standard power level at which control cells with the strongest fluorescence intensity verged on a saturated signal (i.e., fluorescence intensity of <250). This ensured that the signal intensity values measured for all other cells were below the saturated level and could be accurately determined. All measurements were conducted with identical settings, e.g., magnification, photomultiplier tube gain and offset, pinhole size, and averaging. A maximum projection of each cell was obtained from a standard-thickness six-section scan, and the mean maximum intensity was measured.

Immuno-EM. Doubly synchronized control, SBP-treated, and biotinylated SBP-treated (710 μM) parasites were first rinsed in RPMI (without serum) and then aliquoted into 200-μl Eppendorf tubes. Cells were centrifuged (1,000 rpm, 2 min), the supernatant was discarded, and the pellet was then resuspended in 150 μl of 4% paraformaldehyde and 0.5% glutaraldehyde in RPMI (stock solutions of 16% EM-grade paraformaldehyde and 25% glutaraldehyde [Electron Microscopy Sciences]) at pH 7.4. Cells were then microwave processed for 2 min at 15 W, followed by 2 min at 0 W (cooling step) and a further 2 min at 30 W, using a Leica EM AMW microwave processor (Leica Microsystems). Once fixed, cells were again centrifuged, the supernatant was discarded, and the pellet was resuspended in RPMI. Following another centrifugation step and removal of supernatant, the remaining pellet was pipetted into an Eppendorf tube containing a 58°C solution of 1.2% DNA-grade agarose, briefly centrifuged, and then cooled on ice to set. Once the agarose set, a razor was used to cut the Eppendorf tube away from the set agarose, and small, <1-mm^3 sample blocks of the fixed cells in agarose were cut. Sample blocks were further microwave processed using serial ethanol dehydration with 10, 25, 50, 75, 90, and 100% steps (1 min each at 20 W) followed by serial ethanol-LR White resin infiltration with 10, 30, 50, 75, 100, 100, and 100% resin steps (3 min each at 12 W). Samples in 100% resin were heat polymerized (58°C) overnight. Hardened blocks were sectioned using a diamond knife (Delaware Diamond Knives) on a Leica Ultracut R microtome (Leica Microsystems), and sections were collected on single-slot gold or copper-palladium grids (Pro Sci Tech). The sections were immunolabeled with SERA5 MAb 2F3 (3.6 mg/ml) at a dilution of 1:200 (in PBS overnight at 4°C), followed by a serial wash and subsequent labeling with either 18-nm colloidal gold–goat anti-mouse beads (1:400; Jackson ImmunoResearch) or 10-nm colloidal gold-streptavidin (1:100; Sigma) for 1 h at 36°C, followed by further contrast staining with 2% aqueous uranyl acetate. Sections were examined using a Philips CM120 electron microscope at 120 kV, and images were recorded using a Gatan model 791 multiscan charge-coupled device camera. Images were further processed and plates arranged using Adobe Photoshop.

RESULTS

Expression, purification, and characterization of SERA proteins. High-quality recombinant SERA central domain fragments were required for phage panning, antibody production, and use in binding assays. SERA4 and -5 fragments were oxidatively refolded from the reduced and denatured starting material by in vitro methods, as described previously (22). In general, the refolded material eluted earlier from an RP-HPLC column than the denatured starting material did (Fig. 2a to c), indicative of a change in protein conformation and consistent with protein refolding. Furthermore, differential migration of the soluble refolded material under reducing and nonreducing conditions by SDS-PAGE is indicative that the refolded proteins are monomers with a disulfide-bond-stabilized conformation (Fig. 2a to c, insets).

Feasibility of selective targeting of SERA5 enzyme domain. Since the central enzyme domains of the most abundant blood-stage SERA proteins, SERA4, -5, and -6, possess relatively high sequence identities (66% between SERA5E and -4E and 56% between SERA5E and -6E), we initially assessed the feasibility of generating reagents specific for this region. Accordingly, antibodies were raised to purified recombinant SERA5E and, as a rigorous test of specificity, examined for the ability to recognize proteins derived from solubilized parasites that were separated by SDS-PAGE, with or without reducing agent in the sample buffer. Electrophoresis of nonreduced samples for extended periods after the dye front left the gel resulted in differential migration of the various parasite-derived SERAs, which can be discerned following immunoblotting (30).

The identities of bands corresponding to parasite-derived SERA4, -5, and -6 were confirmed using antibodies raised against unique sequences in the N-terminal regions of the corresponding SERA proteins (Fig. 3a, lanes A to C). Clear differences were observed in the migration of these proteins under nonreducing conditions, but the observed resolution between these proteins was lost when SDS-PAGE was conducted under reducing conditions (Fig. 3b).

Importantly, polyclonal antibodies and MAbs raised to recombinant enzyme domain fragments of SERA5 were found to specifically recognize parasite-derived SERA5 electrophoresed under nonreducing conditions (Fig. 3, lanes G to I). Furthermore, polyclonal antibodies targeting the same region in SERA4 were similarly specific for SERA4 (Fig. 3, lane E). Together, these results indicate that despite the high level of sequence identity found in the enzyme domains of various *P. falciparum* SERAs, sufficient sequence and/or structural differences exist to enable their specific targeting.

Panning of phage display libraries. Since it is likely that future antimalarial agents that target the SERAs will be small organic molecules, we also attempted to generate reagents of a much smaller molecular size than that of antibodies that could specifically recognize the enzyme domain of SERA5E. Hence, phage display was used to identify short peptides that bound specifically to recombinant SERA5E. In these experiments, two pools of phage-displayed peptide libraries were used for panning. Both pools contained a mixture of linear and cyclic peptide sublibraries of either 8 or 14 residues in length, displayed as fusions to the M13 gene VIII coat protein.

In the cyclic libraries, a pair of cysteine residues were fixed at different positions, with the remaining residues randomly mutated, while in the linear libraries, all residues were randomized. The level of molecular diversity of each individual

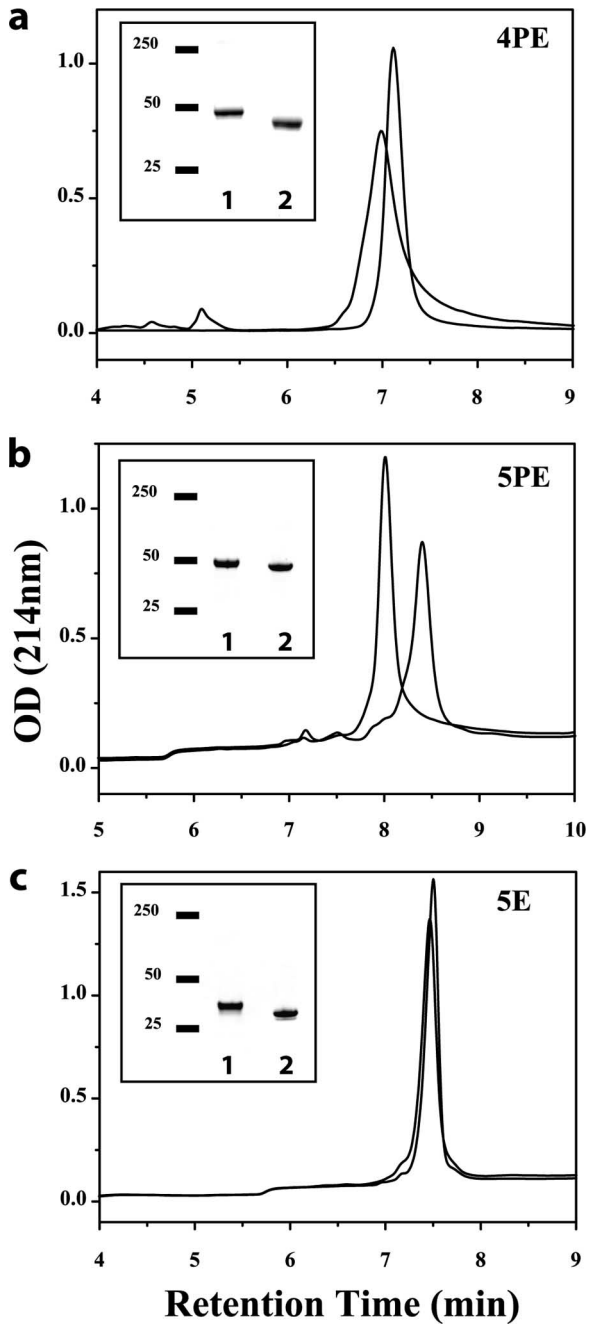

FIG. 2. RP-HPLC and SDS-PAGE characterization of the various SERA central domain fragments used in this study. RP-HPLC profiles for various SERA domain fragments (SERA4PE [a], SERA5PE [b], and SERA5E [c]) were obtained using a gradient of 0 to 100% buffer B from 0 to 12 min at a flow rate of 0.5 ml/min on a C_8 2.1 (internal diameter)- by 100-mm column (buffer A was 0.05% [vol/vol] trifluoroacetic acid, and buffer B was 0.05% [vol/vol] trifluoroacetic acid in acetonitrile). Each graph is an overlay of the chromatograms obtained before and after refolding. The earlier eluting peak for SERA4PE, -5PE, or -5E (a to c) contains the refolded protein. Insets show the SDS-PAGE Coomassie-blue stained gels for each protein fragment, either in the presence of reducing agent (lanes 1) or without the reducing agent (lanes 2) in the sample buffer. The locations of molecular weight standards are indicated on the left side of each gel. OD, optical density.

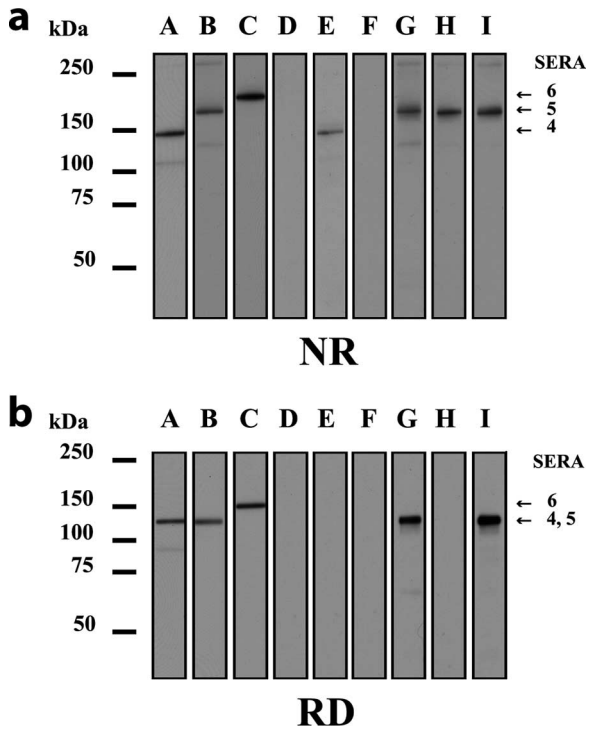

FIG. 3. Reagents targeting specific SERA enzyme domains can be generated. Magnet-purified 3D7 parasite material was electrophoresed with (a) or without (b) reducing agent in the sample loading buffer until the 50-kDa marker had reached the bottom of the gel. Proteins were then blotted onto polyvinylidene difluoride membranes and probed with a panel of antibodies raised to SERA4, -5, and -6. Lanes A, B, and C were probed with rabbit polyclonal antibodies raised to regions of unique linear protein sequence in the 47-kDa N-terminal domains of SERA4, -5, and -6, respectively (12). Lanes D and E were probed with prebleed serum and rabbit polyclonal antibodies raised to the in vitro-refolded SERA4 central domain fragment, respectively. Lanes F and G were probed with prebleed serum and rabbit polyclonal antibodies made to the in vitro-refolded SERA5 central domain fragment, respectively. Lanes H and I were probed with MAbs 3E8 and 2F3, which react with epitopes within the SERA5 enzyme domain. MAb 3E8 recognizes a disulfide-bond-stabilized conformational epitope, while MAb 2F3 recognizes a linear surface-exposed epitope.

library was estimated to range between 10^8 and 10^{10} peptide sequences.

Following six rounds of panning, 48 individual clones from each pool were propagated and tested for the ability to bind to SERA5. All of the clones from the 8-residue library were positive (optical density at 450 nm of >1.5) and displayed essentially no binding to the blocking protein, while approximately one-third of the clones from the 14-residue library pool were positive. From these positive clones, approximately 16 from each library pool were selected and sequenced to determine the identities of the displayed peptides. In the case of the clones from the 8-residue libraries, the same peptide sequence (HCWHYKFC [SBP7]) was present in every clone sequenced (Table 1), while in the 14-residue libraries a number of different peptide sequences were obtained (SBP1-6), with multiple copies of some of the sequences observed (Table 1). In addition, the different positions of the cysteine residues in these

TABLE 1. SERA5 binding sequences selected from naïve libraries[a]

SBP	Sequence (no. of clones with sequence)
SBP1	LVCHPAVPALLCAR (1)
SBP2	RCCAPYVPAFFCEC (1)
SBP3	SRAVCPVEVCRWVV (3)
SBP4	FRAVCPPAVCYWHS (3)
SBP5	EGWCEMHSRWCVVS (3)
SBP6	SVYCEKFRWVCEFR (3)
SBP7	HCWHYKFC (16)

[a] The sequences shown are from all clones sequenced following six rounds of panning.

sequences suggested that each peptide had emerged from different sublibraries within the pool.

Closer examination of the 14-residue peptide sequences indicated strong similarities between some of the peptides. In particular, peptide sequences 1 and 2 contained the motif XXCXPXVPAϕϕCXX (where X represents any amino acid and ϕ represents a hydrophobic residue), while peptide sequences 3 and 4 contained the motif XRAVCPXXVCXWXX.

Affinities of SBPs. To determine the relative affinities of peptides binding SERA5, each peptide sequence was first subcloned into a gene III phage display vector. Display via gene III eliminates the problem of avidity effects associated with display through the high-copy-number gene VIII coat protein.

Purified phage preparations for each of the gene III-fused peptides were titrated and tested for the ability to bind to immobilized SERA5E in an ELISA. Only very weak signals (at the lowest dilutions) were observed for each sequence except SBP1, which suggested that it bound to SERA5E with a significantly higher affinity than those of the other peptides (Fig. 4a). No binding was observed for several irrelevant peptides of various lengths displayed as gene III fusions (Fig. 4a). Since peptide sequences SBP2 to -7 had apparently low affinities for SERA5, they were not investigated further.

To determine the affinity of SBP1 for SERA5, a variety of competition ELISAs were performed. In the first, SERA5E was immobilized onto the plate and binding to phage-displayed SBP1 was competed with either soluble SERA5E or a synthetically derived form of the cyclic SBP1 peptide. Over several experiments, the 50% inhibitory concentration (IC_{50}) measured was consistently on the order of fivefold lower (approximately 200 nM versus 1 μM) when the protein was used as competitor than when the synthetic peptide was used (Fig. 4b). When the experiments were repeated using the longer SERA5PE protein (which is comprised of the pro- and enzyme domains of SERA5) immobilized on the plate, the IC_{50} observed with the synthetic peptide competitor (890 nM) was very similar to that observed for immobilized SERA5E (Fig. 4b). However, when the SERA5PE protein was used as a competitor in this experiment, the affinity was somewhat lower (IC_{50} = 1.7 μM) (Fig. 4). Combined, these results suggest that the affinities of SBP1 for immobilized proteins (SERA5PE versus SERA5E) are very similar, while for proteins in solution the affinity for the shorter SERA5E protein is higher than that for SERA5PE.

Analysis of specificity of SBP1 binding to SERA5. To examine the specificity of the interaction between SBP1 and SERA5E, the gene III-displayed peptide was tested in an ELISA for the ability to bind to various forms of the recombinant enzyme domains from SERA5 and SERA4, the only other SERA for which we can produce a correctly folded recombinant protein. SERA4 possesses high amino acid sequence identity with SERA5 throughout the enzyme domain and, like SERA5, belongs to the "serine-type" SERA group.

Although the phage-displayed SBP1 peptide readily recognized the refolded SERA5 fragment in this assay, as demonstrated by a strong titration signal, the same peptide failed to recognize either refolded or reduced and alkylated fragments of SERA4 (Fig. 4c). Moreover, SBP1 was also unable to bind the reduced and alkylated form of SERA5E, indicating that the protein-peptide interaction was dependent upon the disulfide-bond-stabilized conformation of SERA5 (Fig. 4c).

The binding of SBP1 to SERA5 was found to be further dependent upon the peptide's cyclic conformation, which is stabilized by a single intramolecular disulfide bond. Hence, in competition ELISAs, the reduced and alkylated SBP1 synthetic peptide could not outcompete the gene III-displayed peptides binding to immobilized SERA5E. In fact, no competition was observed, even at the highest competitor concentration (70 μM) tested (data not shown).

These results indicate that SBP1 binds specifically to SERA5 (though the limited number of recombinant SERA proteins available for testing presently limits our analysis) and demonstrate that the correct disulfide-bonded conformations of both the protein and peptide are critical for the interaction.

SBP1 localizes to the parasitophorous vacuole in fixed parasite cells. It was previously determined using immuno-EM (24) and confocal microscopy (7) that SERA5 localizes to the parasitophorous vacuole in trophozoites and schizonts. Although SERA5 has no obvious glycosylphosphatidylinositol anchor motif or transmembrane spanning region, studies utilizing antibodies targeting the N-terminal 47-kDa domain (Fig. 1) have shown that the molecule remains associated with the merozoite surface postrupture (7). To assess whether SBP1 could target SERA5 within a parasite, a biotinylated form was used in confocal microscopy studies. The peptide was found to colocalize with SERA5 in a manner similar to that of MAb 3E8 (Fig. 5), which recognizes a conformational disulfide-bond-dependent epitope within the SERA5 enzyme domain (Fig. 3). Late trophozoites (Fig. 5A) and schizonts (Fig. 5B) probed with either biotinylated SBP1 (Fig. 5, column 1) or MAb 3E8 (Fig. 5, column 2) produced fluorescence patterns that showed substantial overlap (Fig. 5, column 4), confirming the colocalization of SBP1 and SERA5.

SBP1 delays rupture in late-stage parasites in both a dose- and conformation-dependent manner. Since SBP1 was found to localize with SERA5 in fixed late-stage parasites, we next assessed the effect of the peptide on parasite growth in culture. The addition of increasing amounts of cyclized SBP1 to doubly synchronized cultures of *P. falciparum* strain 3D7 parasites (32 h) resulted in a direct linear accumulation of late-stage parasites that had not ruptured 6 h after ring-stage parsites were first detected in the control cultures (Fig. 6). Notably, when the same peptide was carboxymethylated to remove the constraining influence of the disulfide bond, no accumulation of late-stage parasites was observed over the same concentration range. Instead, parasites incubated in the presence of the modified SBP1 peptide transitioned to ring stages at approximately

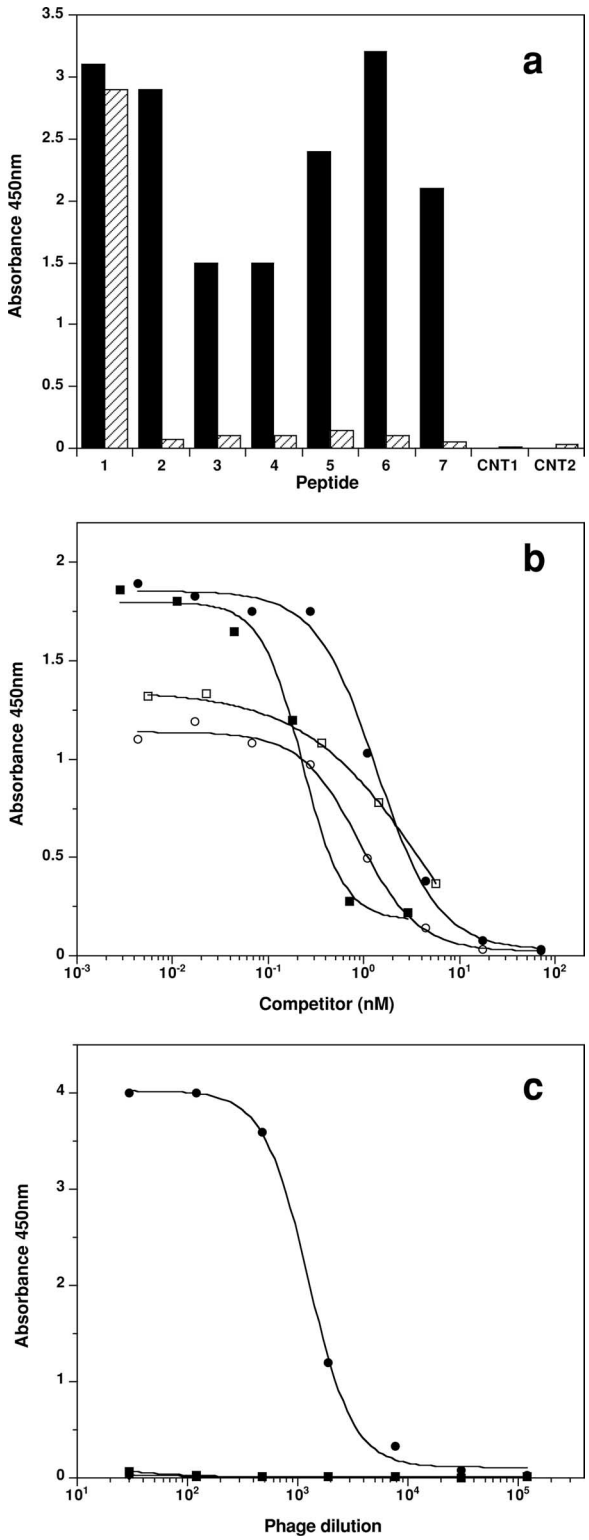

FIG. 4. Biochemical analysis of SBP1. (a) SBP1 displayed on M13 gene VIII and gene III binds SERA5. Binding of representative clones expressing each of the SBPs as gene VIII fusions (supernatant diluted 1:3) (black bars) or gene III fusions (purified phage diluted 1:10) (hatched bars) was measured by ELISA. Only SBP1 fused to gene III binds SERA5. (b) Determination of the affinity of binding of SBP1 to SERA5. The binding affinities of SBP1 for various SERA5 constructs were determined using competition ELISA. Assays were performed with the phage-displayed peptide interacting with immobilized recombinant SERA5E (solid symbols) or SERA5PE (open symbols). The competitors were synthetic SBP1 (open and closed circles), SERA5E (solid squares), and SERA5PE (open squares). (c) Specificity of SBP1 binding to SERA5. SBP1 binding to SERA5E (circles), SERA4PE (squares), reduced/alkylated SERA5E (diamonds), and reduced/alkylated SERA4PE (triangles) was examined by a direct binding ELISA. Each protein was used to coat a 96-well plate at a fixed concentration, and binding of SBP1 displayed on M13 phage was determined. Only nonreduced SERA5 binds to SBP.

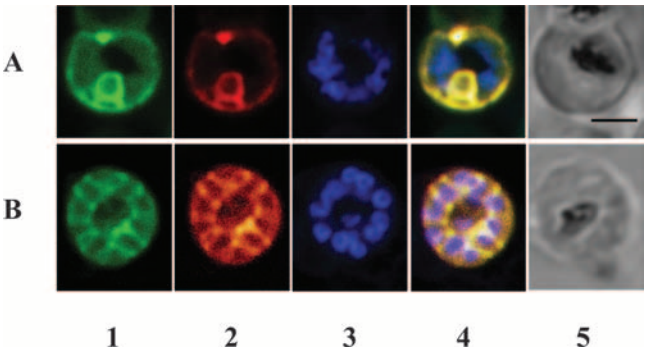

FIG. 5. SBP1 colocalizes with SERA5 within the parasitophorous vacuole of mature blood-stage parasites. Late trophozoites (A) or schizonts (B) were probed with biotinylated SBP1 (column 1; green) and MAb 3E8 (column 2; red). Parasite nuclei (column 3) were stained (blue) using the DNA stain Hoechst 33258. Areas of colocalization for SBP1 and SERA5 are observed as yellow areas (column 4) in the superimposed fluorescence patterns for biotinylated SBP1 and MAb 3E8. The transmission images of parasites viewed using light microscopy are shown in column 5. Bar, 2 μm.

the same rate as control parasites to which no peptide was added (Fig. 6).

The percentage of retention of late-stage parasites observed for the highest SBP1 concentration investigated (710 μM) was similar in magnitude to that caused by several protease inhibitors (E64 and a 1:1 mixture of antipain and leupeptin) used at concentrations known to compromise the parasite rupture/release process (56% ± 6% and 28% ± 4% late-stage parasites remaining following treatment with 10 μM E64 and 10 μM antipain-leupeptin, respectively) (28, 34, 42).

Kinetics of accumulation of late-stage parasites incubated with SBP1. Given that the level of accumulation of late-stage parasites was found to be significant when SBP1 was used at high dosages (Fig. 6), we further investigated the effect of the peptide on parasite development over time (Fig. 7). Parasites were incubated in culture medium containing either SBP1, the reduced and alkylated form of SBP1 (both at 710 μM), or PBS. The number of accumulated late-stage parasites was determined at 3-h intervals over a 12-h period after ring-stage parasites were first detected in the control cultures.

Over most of the time course, the numbers of accumulated late-stage parasites in cultures incubated with SBP1 remained significantly greater than those detected in control cultures (i.e., those treated with reduced/alkylated SBP1 or PBS). The maximum differences between these curves were observed between 3 and 9 h after rupture of the control parasites, and the

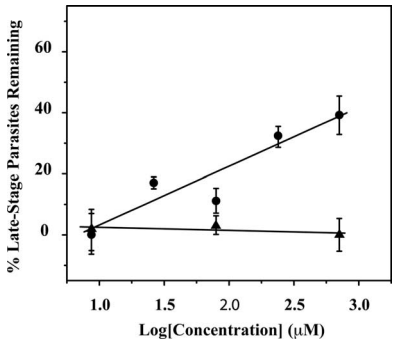

FIG. 6. SBP1 causes an accumulation of *P. falciparum* strain 3D7 late-stage parasites. Parasites were cultured until approximately 6 h postrupture, as determined by the first appearance of ring-stage parasites in control (PBS) cultures. Percentages of late-stage parasites remaining were calculated by subtracting the values obtained for the PBS control cultures from those obtained for either the SBP1 (circles)- or reduced and alkylated SBP1 (squares)-treated cultures. Mean and standard error of the mean (SEM) values were determined from at least triplicate experiments.

relative delay period (i.e., the time taken for SBP1-treated parasites to reach an equivalent percentage of late-stage parasites to that determined for the control cultures) was estimated to be approximately 6 h (Fig. 7a). A similar delayed time course was also observed for D10 parasites, another cultured strain of *P. falciparum*, grown in the presence of SBP1 (Fig. 7b). Beyond 12 h postrupture, the numbers of late-stage parasites in cultures treated with SBP1 approached zero and approximated the numbers of parasites of a similar stage observed in the control cultures (Fig. 7a and b).

We also examined the effect of SBP1 on the D10 *sera4* knockout line (29) (Fig. 7c). SERA4 belongs to the "serine-type" SERA subgroup (7, 22), as does SERA5, and is the next most strongly expressed member of the SERA family in wild-type blood-stage parasites (30). In these experiments, a more pronounced effect on the rupture process of these compromised parasites would be anticipated if the functions of both SERA4 and SERA5 were degenerate. However, the similar outcomes obtained for the *sera4* knockout and wild-type parasites suggest that there may not be a high level of degeneracy in the function of various SERAs from the same (serine-type) subgroup, though further investigation is required to more reliably establish this observation.

The effect of SBP1 on the intraerythrocytic development of late-stage parasites was also reflected in the subsequent ring-stage parasitemias (Fig. 8). Although the percentages of parasitemia for both the SBP1- and the reduced and alkylated SBP1 (control)-treated parasites were found to increase with time, the SBP1-treated parasites were found to be approximately 50 to 70% of the ring-stage parasitemias for the control parasites at each time point.

SBP1 interferes with the intraerythrocytic development of late-stage parasites. Confocal microscopy was used to obtain further insight into the nature of late-stage parasites that had accumulated due to treatment with SBP1. Antibodies specific to SERA5 and targeting the central enzyme domain (MAb 3E8) (Fig. 9a, rows a and c) or the C-terminal 18-kDa domain (anti-5P18) (Fig. 9a, rows b and d) were used in conjunction

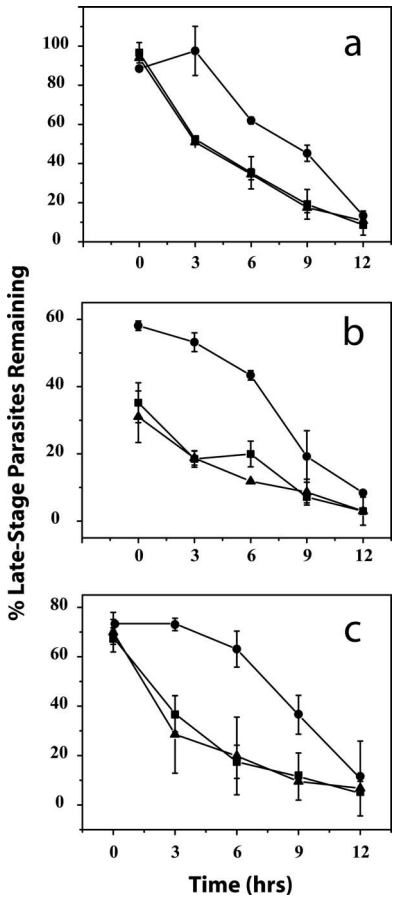

FIG. 7. Time course analysis of the effect of SBP1 on late-stage parasite numbers. *P. falciparum* strains 3D7 (a), D10 (b), and D10 *sera4* knockout (c) were cultured in the presence of SBP1 (●), reduced and alkylated SBP1 (▲), or PBS (■). The time that ring-stage parasites were first detected by microscopy in the control cultures was called 0 h. Parasite cultures were sampled every 3 h for 12 h from this time point. SBP1 and reduced and alkylated SBP1 were used at a concentration of 710 μM. The mean and SEM calculated for each data point were determined from at least triplicate experiments.

with a fluorescent DNA stain (Hoechst 33258) (Fig. 9a and b) to determine the distribution of SERA5 and the number of nuclei within SBP1-treated parasites. At the 54-h time point (i.e., 6 h after the detection of the first ring-stage parasites in the control cultures), parasites were found to have a SERA5 fluorescence pattern of much weaker intensity than that seen for the control parasites. In fact, a considerable increase in the gain function of the photomultiplier tube on the confocal microscope was required to view the fluorescence patterns for these compromised parasites (Fig. 9b, compare top and bottom rows). While the observed fluorescence patterns were variable, many of these parasites exhibited a partial "rim-like" appearance, as seen in late trophozoite stages (for example, see Fig. 9a, rows a and b). Most compromised parasites also failed to exhibit a fluorescence pattern that surrounded developing merozoites, as typically seen in control schizonts when the parasitophorous vacuole fills with merozoites (for example, see Fig. 9a, rows c and d).

The fluorescence intensity values obtained for parasites

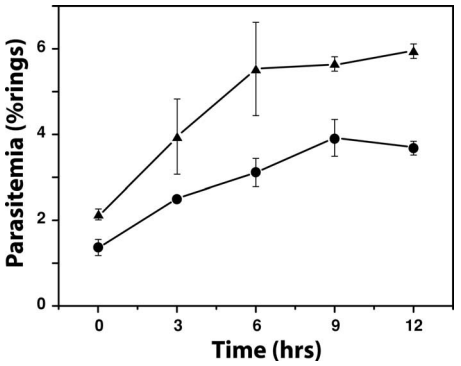

FIG. 8. Time course analysis of the effect of SBP1 on ring-stage parasitemia. 3D7 trophozoites at 2% parasitemia were incubated with 710 μM SBP1 (●) or 710 μM reduced and alkylated SBP1 (▲). The time at which ring-stage parasites were first detected, using microscopy, in the reduced and alkylated control cultures was called 0 h. Parasite cultures were then sampled every 3 h for 12 h. Values represent the means and SEM calculated from at least triplicate experiments.

probed with MAb 3E8 and anti-5P18 were used to semiquantitatively demonstrate that SERA5 levels in the SBP1-compromised parasites were significantly lower than those found in control parasites (Fig. 9c). Since anti-5P18 was raised against the C-terminal domain of SERA5, its binding to SERA5 is unlikely to be inhibited by SBP1 (which targets the enzyme domain), and hence, the reduced signal reflects lower SERA5 levels. However, when the SBP-treated parasites were probed with MAb 3E8, which targets the enzyme domain of SERA5, not only was the fluorescent signal lower than that of the control parasites (Fig. 9c), but it was also lower than that obtained with anti-5P18, suggesting that in this case SBP1 may be inhibiting interaction with MAb 3E8. This is consistent with competition ELISA studies demonstrating that SBP1 can inhibit MAb 3E8 binding to SERA5 (data not shown) and provides further evidence for the specificity of SBP1's biological activity.

The numbers of nuclei observed within control and SBP1-treated late-stage parasites were compared at 48 h and 54 h (i.e., 0 and 6 h, respectively, after the detection of the first ring-stage parasites in the control cultures). These data provide a cross-sectional view of the effect that SBP1 has on the intraerythrocytic development of compromised parasites (Fig. 10). At 48 h, approximately equal numbers of late-stage parasites were observed (Fig. 10a) for both control and SBP1-treated late-stage parasites. However, most control parasites were comprised of greater than eight nuclei per parasite, whereas parasites grown in the presence of SBP1 largely contained three or four nuclei per parasite. At 54 h, a time at which significant accumulation of late-stage parasites was observed in SBP1-treated cultures (Fig. 7), a large increase in late-stage parasites containing three or four nuclei was observed, while the control schizonts decreased in number due to rupture (Fig. 10b). Presumably, the arrested parasites did undergo rupture, possibly due to premature cell death, as their numbers decreased significantly toward the end of the time course (Fig. 7).

Interestingly, viable merozoites were still being produced in the SBP1-treated parasites. We think that these may have been derived from a population of parasites that possessed more than six nuclei. It seems that these parasites may not be compromised developmentally, enabling progression to ring-stage parasites (Fig. 10c and d and Fig. 8). Such parasites may have been able to complete schizogony, possibly because they were more mature at the time of SBP1 addition to cultures.

In order to further investigate the effect of SBP1 on live parasites from culture, we attached a biotin moiety to the N-terminal amine group of the peptide. This peptide was found to affect parasite intraerythrocyte development in a manner similar to that of the unmodified peptide, with the majority of late-stage parasites found to contain two to five nuclei 54 h into the life cycle (Fig. 11a). The majority of the control parasites were comprised of more than eight nuclei, as shown at the 44-h time point (Fig. 11a), with the majority of these late-stage parasites being ruptured before the 54-h time point (data not shown).

Parasites that were grown in the presence of the biotinylated form of SBP1 were then investigated using immuno-EM. The distribution of avidin-gold particles was found to be localized to the parasitophorous vacuole and parasite cytosol in compromised parasites (Fig. 11b, top and bottom rows). Indeed, the localization of biotinylated SBP1 was very restricted, and additional gold particles were not found in the erythrocyte cytosol of infected parasites or in uninfected erythrocytes cultured in the presence of the peptide (data not shown). Infected and uninfected erythrocytes not incubated with the peptide also were not labeled with the avidin-gold particles (data not shown). Moreover, parasites cultured with biotinylated SBP1 and then probed with MAb 2F3 (reactive with the enzyme domain of SERA5), followed by an anti-mouse gold particle conjugate, revealed the presence of SERA5 in both the parasitophorous vacuole and parasite cytosol areas, whereas in untreated parasites, SERA5 was generally restricted to the parasitophorous vacuole (Fig. 11b, top row).

DISCUSSION

Due to their abundance, distribution in the parasitophorous vacuole, and time of expression late in blood-stage development, the SERAs have for some time been implicated in the processes of intraerythrocytic development, rupture, and/or merozoite release from mature schizonts. Recently, we demonstrated that an enzyme domain within the SERA5 molecule has activity on nonphysiological peptidyl substrates under in vitro conditions (22). This outcome suggests that SERA5 has the potential to act upon parasite/host substrates within infected erythrocytes in a similar manner.

This hypothesis is consistent with the outcomes of previous studies demonstrating that serine/cysteine protease inhibitors, such as E64 (34) and antipain-leupeptin (42), can inhibit the release/rupture process(es). However, such compounds generally have broad-range specificities, with the potential to inhibit the functions of a large number of intra- or interclass proteases. Hence, the observed effects of these protease inhibitors could not be restricted to individual molecules such as the SERAs. A more specific approach has been to use anti-SERA antibodies. While these have similarly been shown to have an effect on the parasite rupture/release process, their mechanism of action is not obvious, as they do not target epitopes within

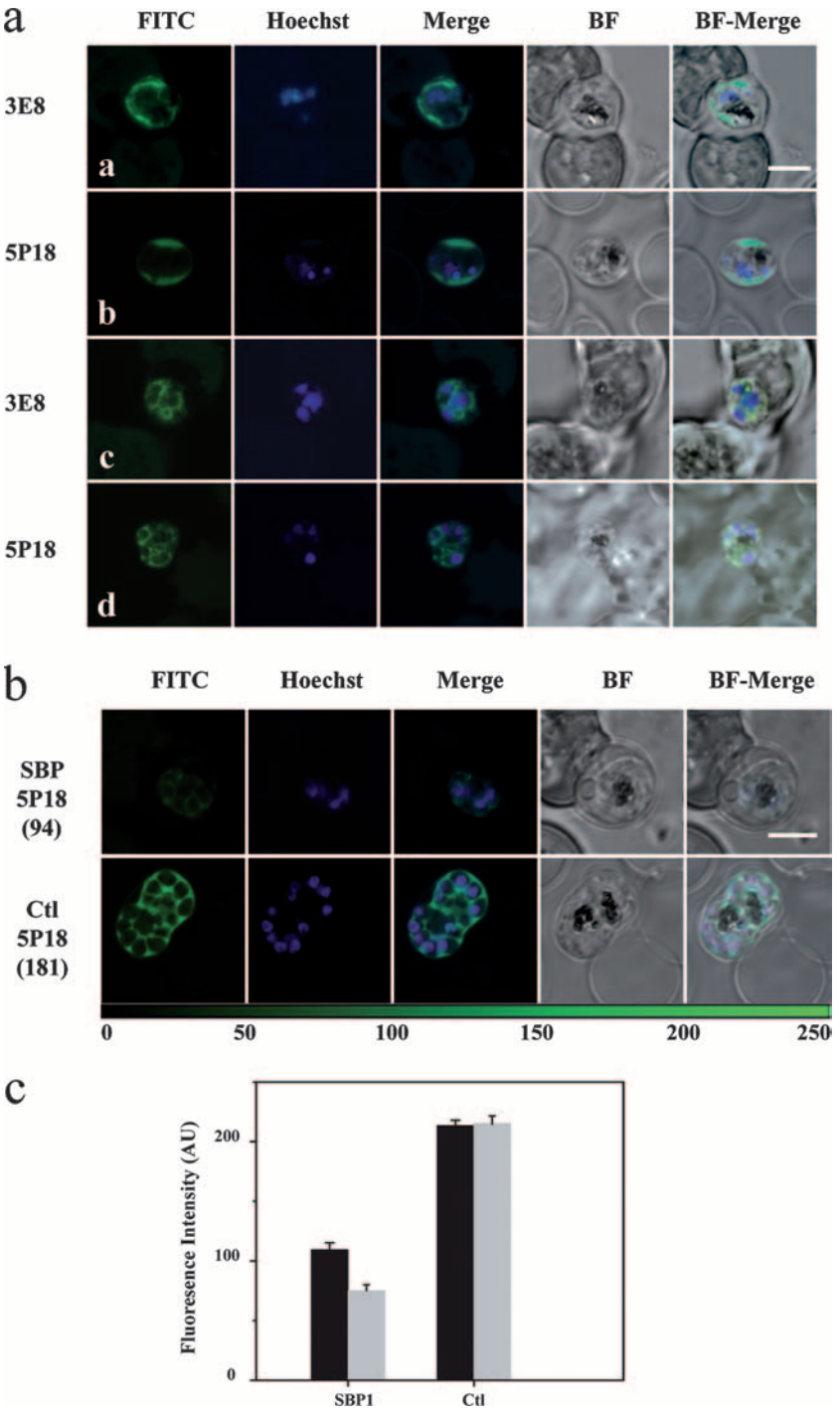

FIG. 9. Confocal microscopy of late-stage strain 3D7 parasites treated with SBP1. (a) Parasites were observed at a time equivalent to 54 h during the extended parasite cycle following SBP1 (710 μM) treatment. Cells were probed with either anti-SERA5 MAb 3E8 (3E8) or rabbit anti-SERA5 P18 domain (C-terminal domain) (5P18) and stained with FITC-labeled anti-immunoglobulin secondary antibodies (green) and the fluorescent DNA stain (blue) Hoechst 33258. Transmission bright-field images (BF) of parasites and the merge of transmission and fluorescent images (BF-Merge) are shown in the last two columns. Bar, 5 μm. Note the "rim-like" distribution of SERA5 in rows a and b stained with different antibodies and the presence of four nuclei in both parasites. In rows c and d, there is a partial distribution of SERA5 around a few developing merozoites and, again, just three or four nuclei are observed. (b) Parasites cultured with (upper row) and without (lower row) SBP1 were probed with polyclonal rabbit antibody 5P18, and images were taken at standardized settings on a confocal microscope. A scale which relates the observed fluorescence intensities of FITC-labeled parasites as a color scale to digital values (i.e., fluorescence intensity values) assigned by the confocal microscope software is shown at the bottom. The fluorescence intensity value calculated for each example of a FITC-labeled parasite is displayed in parentheses at the beginning of each row. Bar, 5 μm. (c) Comparison of mean fluorescence intensity values determined for parasites cultured with and without 710 μM of SBP1. Fluorescence intensity quantifications were performed with standardized settings on a confocal microscope (see Materials and Methods). The mean fluorescence intensity values (arbitrary units [AU]) obtained for SBP1-treated parasites and control parasites probed with anti-5P18 polyclonal antibody are shown as black bars, and those for parasites probed with MAb 3E8 are shown as gray bars. Randomly selected parasites from multiple fields were used to determine the mean (and SEM) fluorescence intensity values ($n > 30$).

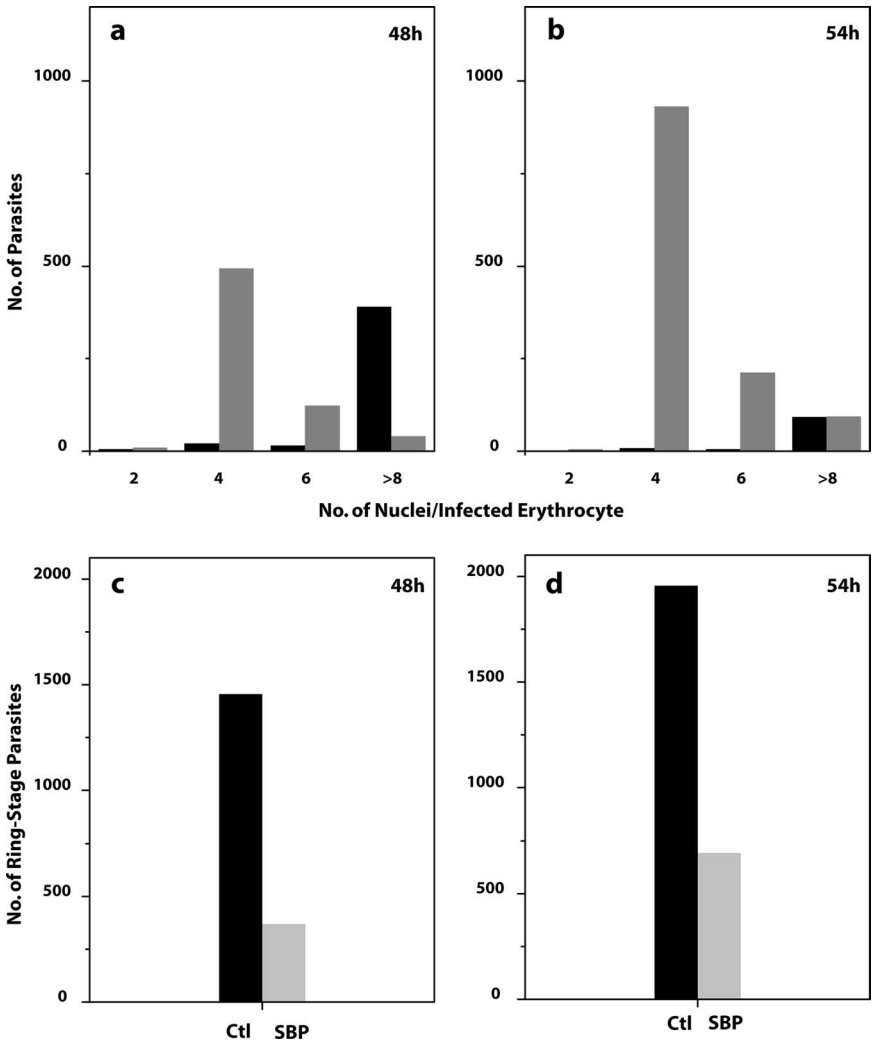

FIG. 10. Treatment with SBP1 affects numbers of nuclei and ring-stage parasites. The graphs show quantitation of the number of nuclei/infected erythrocyte (a and b) and the number of ring-stage parasites (c and d) for parasites obtained from control (black) and SBP1-treated (710 μM) (gray) cultures at time intervals 48 h (a and c) and 54 h (b and d) within the extended parasite cycle. Total parasite numbers are shown for a single set of experiments. Late-stage parasites were differentiated from ring-stage parasites by observation of the food vacuole. The time that ring-stage parasites were first detected by microscopy in the control cultures was called 48 h. Parasite numbers were determined for an identical number of microscope fields viewed for both SBP1-treated and control parasites. Nuclei were stained with Hoechst 33258 and viewed using a confocal microscope, as described in Materials and Methods.

the enzyme domain (31, 32). Furthermore, because of their multivalency and large size, the observed inhibitory activity may be a consequence of agglutination, steric hindrance, or some other effect(s). Another, more specific strategy for probing SERA protein function is through gene knockout studies. Indeed, Aly and Matuschewski demonstrated that a "cysteine-type" SERA was critical for the release of *Plasmodium berghei* sporozoites from oocytes within the mosquito stage of the parasite life cycle by using a parasite line with this *sera* deleted (2). However, attempts to disrupt the *P. falciparum sera5* gene have to date been unsuccessful.

Specific targeting of SERA5 with short bioactive peptides. In this study, we have demonstrated that two of the abundantly expressed SERAs in blood-stage parasites (SERA4 and -5) have unique surface conformations within their central enzyme domains. This has enabled the targeting of antibody and peptidyl reagents to specific SERAs for functional investigation. In order to determine the importance of SERA5, in particular, in blood-stage development, we generated a small peptide (SBP1) that specifically associated with the enzyme domain of this protein. SBP1 is a 14-residue (1,500-Da) molecule that is cyclized via a disulfide bond and was identified by panning of randomized peptide libraries displayed on the surfaces of phage against SERA5. Although a variety of peptide sequences were identified that bound to SERA5, only SBP1 bound with an affinity (approximately 1 μM) high enough to enable further analysis. The functional effects of SBP1 on late-stage parasites were found to be dependent upon the disulfide-bond-constrained conformation of the peptide and were consistent with the results of our in vitro binding studies, which revealed that the carboxymethylated form was unable to bind SERA5. Furthermore, confocal microscopy demonstrated that

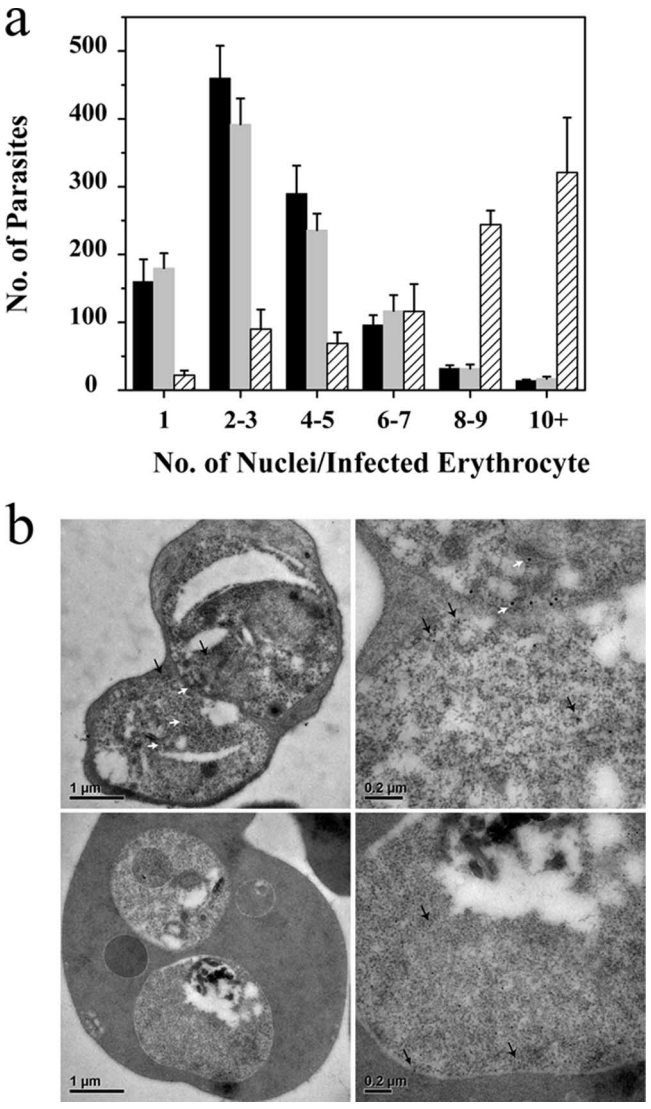

FIG. 11. Biotinylated SBP1 also inhibits intraerythrocytic development of parasites and localizes to the parasitophorous vacuole when cultured with parasites. (a) Quantitation of the number of nuclei/infected erythrocyte for parasites cultured in the presence of 710 μM of either SBP1 (gray bars) or biotinylated SBP1 (black bars) after 54 h (i.e., 6 h after the observation of the first rings in control parasites). The data for control parasites (hatched bars) were taken at 44 h (i.e., prior to the observation of the first rings in the control parasites), as these parasites ruptured before the SBP1-treated parasites. Late-stage parasites were differentiated from ring-stage parasites by observation of the food vacuole. Parasite numbers were determined for an identical number of microscope fields viewed for SBP1-treated, biotinylated SBP1-treated, and control parasites. Nuclei were stained with Hoechst 33258. Data were derived from triplicate independent experiments. (b) Immuno-EM images of synchronized parasites cultured in the presence of biotinylated SBP1 (710 μM). Sections were probed with MAb 2F3 (to detect SERA5) and avidin (to detect biotinylated SBP1) and visualized using 18-nm and 10-nm gold beads, respectively (top row), or probed using avidin and gold beads (10 nm) only (bottom row). Scale bars are indicated, and arrows (white arrows, 18-nm gold beads; black arrows, 10-nm gold beads) are used to assist in viewing some of the gold beads in these sections.

SBP1 had a similar distribution to that of SERA5 within the parasitophorous vacuoles of late-stage parasites, suggesting that it could be used for targeting parasite-derived SERA5 in vivo.

Significantly, treatment of synchronized cultures with SBP1 results in the retention of late-stage parasites at levels similar to those observed for the protease inhibitors E64 and antipain-leupeptin. Parasites cultured in the presence of general protease inhibitors have been reported to progress no further than schizonts and typically form merozoite clusters, which do not progress to the ring stage (28, 34, 42). In contrast, no such clusters were observed in SBP1-treated parasites. Instead, SBP1 was found to affect the intraerythrocytic development of the late-stage parasites, which resulted in their accumulation during time course assays with several cultured strains of *P. falciparum*. Closer investigation revealed that SBP1 severely compromised a subpopulation of parasites, which failed to complete schizogony, resulting in lower ring-stage parasitemias than those observed for control parasites. A second population of possibly more mature parasites were less susceptible to treatment with SBP1, resulting in delayed schizont rupture before progression to the ring stage.

Those parasites that were severely compromised arrested predominantly at the three- to four-nucleus stage of development, with the greatest accumulation of parasites observed between 0 and 6 h after rupture of the control parasites. The times over which large numbers of late-stage parasites accumulated were observed to be similar to those reported for the retention of merozoite bundles by use of protease inhibitors such as chymostatin and leupeptin (28). We found that by 12 to 15 h after rupture of the control parasites, the majority of both subpopulations of compromised parasites had disappeared in the presence of SBP1. This observation is consistent with the disappearance of merozoite bundles from cultures incubated with protease inhibitors over a similar time course (5, 13, 28). Although it was thought that the merozoite bundles disappeared via dissociation (28), we believe that parasites that arrested in the presence of SBP1 did not complete their intraerythrocytic development and went on to rupture rather than dissipate via dissociation.

Further investigation of the late-stage parasites grown in the presence of SBP1, using confocal microscopy, revealed that many contained a residual or incomplete "rim-like" fluorescence typical of the pattern seen in late trophozoites/early schizonts. Furthermore, the fluorescence pattern observed for many of these parasites was not as comprehensive and was of a much lesser intensity than that observed for control parasites at similar stages of the life cycle. A quantitative assessment of the levels of SERA5 present in these arrested parasites supported this observation and revealed that SERA5 levels were significantly lower, perhaps limiting its ability to fulfill its function in parasite development.

The interaction of SBP1 with live parasites was characterized using immuno-EM of parasites that had been cultured in the presence of a biotinylated form of the peptide. The reactivity of the peptide with the parasite-infected erythrocytes was found to be very specific and revealed that the peptide was able to cross the erythrocyte and parasitophorous vacuole membranes to localize in the parasitophorous vacuole, where SERA5 is known to be located. Furthermore, the integrity of

the parasite plasma membrane appears to have been compromised following SBP1 treatment, as both SERA5 and the peptide were also identified in the parasite cytosol, a site where SERA5 is not normally localized. The molecular mechanism behind this event is not known, but these results imply that blocking SERA5 function results in the breakdown of the plasma membrane and eventually the complete rupture of these compromised parasites. Recently, another similar rupture phenotype was observed in parasites that have inducible expression of a mutant form of SERA5 (A. Hodder et al., submitted for publication). This phenotype was generated after mutating a single amino acid (i.e., Ser^{596} to Ala) within the catalytic triad of SERA5 and, again, probably resulted from a loss of function in this protein.

As mentioned previously, not all parasites grown in the presence of SBP1 were severely compromised, and some completed schizogony to release merozoites and produce rings. Similar studies have found that the timing of the addition of compounds such as protease inhibitors to culture can be crucial in determining whether or not schizonts are effectively compromised (19, 28). We know from our studies that if SBP1 was added to cultures once late-stage parasites had begun to divide, then it was much less effective at interfering with the intraerythrocytic development of these parasites (data not shown). These observations may reflect that some time is required before a critical amount of SBP1 is able to cross the erythrocyte and parasitophorous vacuole membranes and arrest the intraerythrocytic development of susceptible parasites.

Future improvements in SBPs. Although numerous peptides were found to bind to SERA5 in the initial phage screens (Table 1), only SBP1 bound with a high affinity. This suggests that significant avidity effects associated with fusion of the peptide libraries to the major M13 coat protein, the gene VIII protein, enabled selection of the other, weaker binding peptides. Alternatively, these other peptides may be expressed poorly when fused to gene III and hence only appear to bind more weakly. It was, however, somewhat surprising that SBP2, which appeared to be related to SBP1 because of the positioning of 8 identical or similar residues out of 14 total residues, appeared to bind with a much lower affinity. The SBP2 sequence was unusual in that it contained two additional cysteine residues compared to SBP1, at positions 2 and 14. It is possible, therefore, that the phage-displayed form of this peptide may exist in a number of conformations, with various combinations of the disulfide linkages (and/or free cysteines) between the four cysteines present. Hence, only a small percentage of the total combinations may be in the "active" conformation, which could account for the weaker binding observed. It may be possible to further improve the affinity of SBP1 for SERA5 through the construction of secondary libraries in which residues are randomized around the sequence motif (XXCXPXV PAϕϕCXX) conserved in SBP1 and SBP2. In the same manner, peptides with increased affinity may also be obtained from secondary libraries based around the conserved motif (XRAV CPXXVCXWXX) observed in SBP3 and SBP4.

The competition ELISA results indicated that SBP1 binding to SERA5 in solution, but not to immobilized SERA5, may be affected by the presence of the N-terminal prodomain. One explanation for this may be that in solution the prodomain is more flexible and can fold over the protein shielding the SBP1 epitope, but when the protein is immobilized onto the plate, the prodomain may be fixed in a more distorted conformation that allows easier access to the SBP1 epitope.

While the potency of the SBP1 peptide is relatively low (i.e., concentrations of >10 μM were required to mediate an effect in parasites), it should also be remembered that in order for the peptide to interact with SERA5, it must cross both the erythrocyte and parasitophorous vacuole membranes. Therefore, the passage of SBP1 through these membranes to access SERA5 may decrease the bioavailability of SBP1 and increase the time required to reach a critical concentration that affects the intraerythrocytic development of parasites. Accessibility to the parasitophorous vacuole could perhaps be improved by coupling the SBP1 peptide (or affinity-matured forms) to membrane-penetrating sequences such as that of Antennapaedia. Again, an affinity-matured form of the peptide or one that is more stably constrained might lead to improvements in potency. If such peptides can be developed from this promising lead molecule, they should provide excellent tools to further elucidate the role of SERAs. This is particularly important given that gene disruption studies of what are perhaps the more important SERAs have to date been unsuccessful.

SERA5 as a drug target candidate. The present results have provided the first real insight into the importance and function of SERA5 in the biology of blood-stage parasites. Furthermore, we have shown that by specifically targeting SERA5, parasite development can be impaired. However, the molecular mechanism(s) by which SBP1 causes parasites to arrest has not been determined, nor have the identities of the residues involved in the association between SBP1 and SERA5 been determined. We recently solved the structure for the SERA5 enzyme domain (Hodder et al., submitted), and structural studies of the SERA-SBP1 complex that are currently under way should resolve this issue and allow us to determine whether SBP1 binds directly within the putative active site, sterically inhibits access to the substrate, or prevents another type of protein-protein interaction outside the catalytic cleft region.

Nevertheless, the present data provide strong evidence that the SERAs should be considered potential antimalarial drug candidates. Since we have now shown that relatively small molecules targeting the enzyme domain of SERA5 are effective at interfering with parasite biology, future studies aimed at the identification of even smaller, more drug-like compounds can now be considered feasible.

ACKNOWLEDGMENTS

This work was funded by an NHMRC of Australia program grant (to B.S.C. and G.I.M.), fellowship (to W.D.F.), and Dora Lush Scholarship (to J.E.M.). B.S.C. and G.I.M. are International Researchers of the Howard Hughes Medical Institute.

We acknowledge Dean Goodman for his assistance in the preparation of parasites for growth assays. We also thank Manuel Baca for provision of phage expression vectors and Peter Colman for critical evaluation of the manuscript. We thank the Australian Red Cross for the supply of blood.

REFERENCES

1. **Aley, S. B., J. A. Sherwood, K. Marsh, O. Eidelman, and R. J. Howard.** 1986. Identification of isolate-specific proteins on sorbitol-enriched Plasmodium falciparum infected erythrocytes from Gambian patients. Parasitology **92:** 511–525.

2. **Aly, A. S., and K. Matuschewski.** 2005. A malarial cysteine protease is necessary for Plasmodium sporozoite egress from oocysts. J. Exp. Med. **202:**225–230.
3. **Aoki, S., J. Li, S. Itagaki, B. A. Okech, T. G. Egwang, H. Matsuoka, N. M. Palacpac, T. Mitamura, and T. Horii.** 2002. Serine repeat antigen (SERA5) is predominantly expressed among the SERA multigene family of Plasmodium falciparum, and the acquired antibody titers correlate with serum inhibition of the parasite growth. J. Biol. Chem. **277:**47533–47540.
4. **Banerjee, R., J. Liu, W. Beatty, L. Pelosof, M. Klemba, and D. E. Goldberg.** 2002. Four plasmepsins are active in the Plasmodium falciparum food vacuole, including a protease with an active-site histidine. Proc. Natl. Acad. Sci. USA **99:**990–995.
5. **Banyal, H. S., G. C. Misra, C. M. Gupta, and G. P. Dutta.** 1981. Involvement of malarial proteases in the interaction between the parasite and host erythrocyte in Plasmodium knowlesi infections. J. Parasitol. **67:**623–626.
6. **Bazan, J. F., and R. J. Fletterick.** 1988. Viral cysteine proteases are homologous to the trypsin-like family of serine proteases: structural and functional implications. Proc. Natl. Acad. Sci. USA **85:**7872–7876.
7. **Bourgon, R., M. Delorenzi, T. Sargeant, A. N. Hodder, B. S. Crabb, and T. P. Speed.** 2004. The serine repeat antigen (SERA) gene family phylogeny in Plasmodium: the impact of GC content and reconciliation of gene and species trees. Mol. Biol. Evol. **21:**2161–2171.
8. **Bzik, D. J., W. B. Li, T. Horii, and J. Inselburg.** 1988. Amino acid sequence of the serine-repeat antigen (SERA) of Plasmodium falciparum determined from cloned cDNA. Mol. Biochem. Parasitol. **30:**279–288.
9. **Carlton, J. M., S. V. Angiuoli, B. B. Suh, T. W. Kooij, M. Pertea, J. C. Silva, M. D. Ermolaeva, J. E. Allen, J. D. Selengut, H. L. Koo, J. D. Peterson, M. Pop, D. S. Kosack, M. F. Shumway, S. L. Bidwell, S. J. Shallom, S. E. van Aken, S. B. Riedmuller, T. V. Feldblyum, J. K. Cho, J. Quackenbush, M. Sedegah, A. Shoaibi, L. M. Cummings, L. Florens, J. R. Yates, J. D. Raine, R. E. Sinden, M. A. Harris, D. A. Cunningham, P. R. Preiser, L. W. Bergman, A. B. Vaidya, L. H. van Lin, C. J. Janse, A. P. Waters, H. O. Smith, O. R. White, S. L. Salzberg, J. C. Venter, C. M. Fraser, S. L. Hoffman, M. J. Gardner, and D. J. Carucci.** 2002. Genome sequence and comparative analysis of the model rodent malaria parasite Plasmodium yoelii yoelii. Nature **419:**512–519.
10. **Contreras, C. E., J. F. Cortese, A. Caraballo, and C. V. Plowe.** 2002. Genetics of drug-resistant Plasmodium falciparum malaria in the Venezuelan state of Bolivar. Am. J. Trop. Med. Hyg. **67:**400–405.
11. **Debrabant, A., and P. Delplace.** 1989. Leupeptin alters the proteolytic processing of P126, the major parasitophorous vacuole antigen of Plasmodium falciparum. Mol. Biochem. Parasitol. **33:**151–158.
12. **Debrabant, A., P. Maes, P. Delplace, J. F. Dubremetz, A. Tartar, and D. Camus.** 1992. Intramolecular mapping of Plasmodium falciparum P126 proteolytic fragments by N-terminal amino acid sequencing. Mol. Biochem. Parasitol. **53:**89–95.
13. **Dejkriengkraikhul, P., and P. Wilairat.** 1983. Requirement of malarial protease in the invasion of human red cells by merozoites of Plasmodium falciparum. Z. Parasitenkd. **69:**313–317.
14. **Delplace, P., B. Fortier, G. Tronchin, J. F. Dubremetz, and A. Vernes.** 1987. Localization, biosynthesis, processing and isolation of a major 126 kDa antigen of the parasitophorous vacuole of Plasmodium falciparum. Mol. Biochem. Parasitol. **23:**193–201.
15. **Fairlie, W. D., A. D. Uboldi, G. J. Hemmings, B. J. Smith, H. M. Martin, P. O. Morgan, and M. Baca.** 2003. A family of leukemia inhibitory factor-binding peptides that can act as antagonists when conjugated to poly(ethylene glycol). Biochemistry **42:**13193–13201.
16. **Gardner, M. J., S. J. Shallom, J. M. Carlton, S. L. Salzberg, V. Nene, A. Shoaibi, A. Ciecko, J. Lynn, M. Rizzo, B. Weaver, B. Jarrahi, M. Brenner, B. Parvizi, L. Tallon, A. Moazzez, D. Granger, C. Fujii, C. Hansen, J. Pederson, T. Feldblyum, J. Peterson, B. Suh, S. Angiuoli, M. Pertea, J. Allen, J. Selengut, O. White, L. M. Cummings, H. O. Smith, M. D. Adams, J. C. Venter, D. J. Carucci, S. L. Hoffman, and C. M. Fraser.** 2002. Sequence of Plasmodium falciparum chromosomes 2, 10, 11 and 14. Nature **419:**531–534.
17. **Gardner, M. J., H. Tettelin, D. J. Carucci, L. M. Cummings, L. Aravind, E. V. Koonin, S. Shallom, T. Mason, K. Yu, C. Fujii, J. Pederson, K. Shen, J. Jing, C. Aston, Z. Lai, D. C. Schwartz, M. Pertea, S. Salzberg, L. Zhou, G. G. Sutton, R. Clayton, O. White, H. O. Smith, C. M. Fraser, M. D. Adams, J. C. Venter, and S. L. Hoffman.** 1998. Chromosome 2 sequence of the human malaria parasite Plasmodium falciparum. Science **282:**1126–1132.
18. **Gor, D. O., A. C. Li, and P. J. Rosenthal.** 1998. Protective immune responses against protease-like antigens of the murine malaria parasite Plasmodium vinckei. Vaccine **16:**1193–1202.
19. **Hadley, T., M. Aikawa, and L. H. Miller.** 1983. Plasmodium knowlesi: studies on invasion of rhesus erythrocytes by merozoites in the presence of protease inhibitors. Exp. Parasitol. **55:**306–311.
20. **Hemingway, J., L. Field, and J. Vontas.** 2002. An overview of insecticide resistance. Science **298:**96–97.
21. **Hodder, A. N., P. E. Crewther, and R. F. Anders.** 2001. Specificity of the protective antibody response to apical membrane antigen 1. Infect. Immun. **69:**3286–3294.
22. **Hodder, A. N., D. R. Drew, V. C. Epa, M. Delorenzi, R. Bourgon, S. K. Miller, R. L. Moritz, D. F. Frecklington, R. J. Simpson, T. P. Speed, R. N. Pike, and B. S. Crabb.** 2003. Enzymic, phylogenetic, and structural characterization of the unusual papain-like protease domain of Plasmodium falciparum SERA5. J. Biol. Chem. **278:**48169–48177.
23. **Kiefer, M. C., K. A. Crawford, L. J. Boley, K. E. Landsberg, H. L. Gibson, D. C. Kaslow, and P. J. Barr.** 1996. Identification and cloning of a locus of serine repeat antigen (sera)-related genes from Plasmodium vivax. Mol. Biochem. Parasitol. **78:**55–65.
24. **Knapp, B., E. Hundt, U. Nau, and H. A. Kupper.** 1989. Molecular cloning, genomic structure and localization in a blood stage antigen of Plasmodium falciparum characterized by a serine stretch. Mol. Biochem. Parasitol. **32:**73–83.
25. **Kunkel, T. A., K. Bebenek, and J. McClary.** 1991. Efficient site-directed mutagenesis using uracil-containing DNA. Methods Enzymol. **204:**125–139.
26. **Li, J., H. Matsuoka, T. Mitamura, and T. Horii.** 2002. Characterization of proteases involved in the processing of Plasmodium falciparum serine repeat antigen (SERA). Mol. Biochem. Parasitol. **120:**177–186.
27. **Luker, K. E., S. E. Francis, I. Y. Gluzman, and D. E. Goldberg.** 1996. Kinetic analysis of plasmepsins I and II aspartic proteases of the Plasmodium falciparum digestive vacuole. Mol. Biochem. Parasitol. **79:**71–78.
28. **Lyon, J. A., and J. D. Haynes.** 1986. Plasmodium falciparum antigens synthesized by schizonts and stabilized at the merozoite surface when schizonts mature in the presence of protease inhibitors. J. Immunol. **136:**2245–2251.
29. **McCoubrie, J. E., S. K. Miller, T. Sargeant, R. T. Good, A. N. Hodder, T. P. Speed, T. F. de Koning-Ward, and B. S. Crabb.** 2007. Evidence for a common role for the serine-type *Plasmodium falciparum* serine repeat antigen proteases: implications for vaccine and drug design. Infect. Immun. **75:**5565–5574.
30. **Miller, S. K., R. T. Good, D. R. Drew, M. Delorenzi, P. R. Sanders, A. N. Hodder, T. P. Speed, A. F. Cowman, T. F. de Koning-Ward, and B. S. Crabb.** 2002. A subset of Plasmodium falciparum SERA genes are expressed and appear to play an important role in the erythrocytic cycle. J. Biol. Chem. **277:**47524–47532.
31. **Okitsu, S. L., F. Boato, M. S. Mueller, D. B. Li, D. Vogel, N. Westerfeld, R. Zurbriggen, J. A. Robinson, and G. Pluschke.** 2007. Antibodies elicited by a virosomally formulated Plasmodium falciparum serine repeat antigen-5 derived peptide detect the processed 47 kDa fragment both in sporozoites and merozoites. Peptides **28:**2051–2060.
32. **Pang, X. L., T. Mitamura, and T. Horii.** 1999. Antibodies reactive with the N-terminal domain of *Plasmodium falciparum* serine repeat antigen inhibit cell proliferation by agglutinating merozoites and schizonts. Infect. Immun. **67:**1821–1827.
33. **Ragge, K., H. H. Arnold, M. Tummler, B. Knapp, E. Hundt, and K. Lingelbach.** 1990. In vitro biosynthesis and membrane translocation of the serine rich protein of Plasmodium falciparum. Mol. Biochem. Parasitol. **42:**93–100.
34. **Salmon, B. L., A. Oksman, and D. E. Goldberg.** 2001. Malaria parasite exit from the host erythrocyte: a two-step process requiring extraerythrocytic proteolysis. Proc. Natl. Acad. Sci. USA **98:**271–276.
35. **Sarkany, Z., and L. Polgar.** 2003. The unusual catalytic triad of poliovirus protease 3C. Biochemistry **42:**516–522.
36. **Sidhu, S. S., H. B. Lowman, B. C. Cunningham, and J. A. Wells.** 2000. Phage display for selection of novel binding peptides. Methods Enzymol. **328:**333–363.
37. **Snow, R. W., C. A. Guerra, A. M. Noor, H. Y. Myint, and S. I. Hay.** 2005. The global distribution of clinical episodes of Plasmodium falciparum malaria. Nature **434:**214–217.
38. **Tonkin, C. J., G. G. van Dooren, T. P. Spurck, N. S. Struck, R. T. Good, E. Handman, A. F. Cowman, and G. I. McFadden.** 2004. Localization of organellar proteins in Plasmodium falciparum using a novel set of transfection vectors and a new immunofluorescence fixation method. Mol. Biochem. Parasitol. **137:**13–21.
39. **Trager, W., and J. B. Jensen.** 1976. Human malaria parasites in continuous culture. Science **193:**673–675.
40. **Vathsala, P. G., A. Pramanik, S. Dhanasekaran, C. U. Devi, C. R. Pillai, S. K. Subbarao, S. K. Ghosh, S. N. Tiwari, T. S. Sathyanarayan, P. R. Deshpande, G. C. Mishra, M. R. Ranjit, A. P. Dash, P. N. Rangarajan, and G. Padmanaban.** 2004. Widespread occurrence of the Plasmodium falciparum chloroquine resistance transporter (Pfcrt) gene haplotype SVMNT in P. falciparum malaria in India. Am. J. Trop. Med. Hyg. **70:**256–259.
41. **White, N. J.** 2004. Antimalarial drug resistance. J. Clin. Investig. **113:**1084–1092.
42. **Wickham, M. E., J. G. Culvenor, and A. F. Cowman.** 2003. Selective inhibition of a two-step egress of malaria parasites from the host erythrocyte. J. Biol. Chem. **278:**37658–37663.
43. **Zhang, M., Z. Wei, S. Chang, M. Teng, and W. Gong.** 2006. Crystal structure of a papain-fold protein without the catalytic residue: a novel member in the cysteine proteinase family. J. Mol. Biol. **358:**97–105.

Editor: W. A. Petri, Jr.